





Surface Functionalization

International Edition: DOI: 10.1002/anie.202001440 German Edition: DOI: 10.1002/ange.202001440

A Benchtop Method for Appending Protic Functional Groups to N-Heterocyclic Carbene Protected Gold Nanoparticles

Joseph F. DeJesus⁺, Lindy M. Sherman⁺, Darius J. Yohannan, Jeffrey C. Becca, Shelby L. Strausser, Leonhard F. P. Karger, Lasse Jensen, David M. Jenkins,* and Jon P. Camden*

Abstract: The remarkable resilience of N-heterocyclic carbene (NHC) gold bonds has quickly made NHCs the ligand of choice when functionalizing gold surfaces. Despite rapid progress using deposition from free or CO₂-protected NHCs, synthetic challenges hinder the functionalization of NHC surfaces with protic functional groups, such as alcohols and amines, particularly on larger nanoparticles. Here, we synthesize NHC-functionalized gold surfaces from gold(I) NHC complexes and aqueous nanoparticles without the need for additional reagents, enabling otherwise difficult functional groups to be appended to the carbene. The resilience of the NHC-Au bond allows for multi-step post-synthetic modification. Beginning with the nitro-NHC, we form an amine-NHC terminated surface, which further undergoes amide coupling with carboxylic acids. The simplicity of this approach, its compatibility with aqueous nanoparticle solutions, and its ability to yield protic functionality, greatly expands the potential of NHC-functionalized noble metal surfaces.

Introduction

While N-heterocyclic carbenes (NHCs) are known to form strong bonds with noble metals, [1] the extreme robustness of NHC self-assembled monolayers (NHC SAMs) was only recently recognized. [2] Following these initial studies, progress has been rapid with NHCs supplanting thiols in applications from catalysis and biosensing to drug delivery [1a,2a,3] because of their enhanced stability and accessibility for chemical modifications. [2d,4] NHC-coated materials are particularly appealing when non-ideal conditions are required, such as large variations in pH or temperature. [1a,2b]

[*] L. M. Sherman, [+] D. J. Yohannan, L. F. P. Karger, Dr. J. P. Camden Department of Chemistry and Biochemistry University of Notre Dame South Bend, IN 46556 (USA) E-mail: jon.camden@nd.edu

Dr. J. F. DeJesus, [+] S. L. Strausser, Dr. D. M. Jenkins Department of Chemistry, University of Tennessee Knoxville, TN 37996 (USA) E-mail: jenkins@ion.chem.utk.edu

J. C. Becca, Dr. L. Jensen Department of Chemistry, The Pennsylvania State University University Park, PA 16802 (USA)

- [+] These authors contributed equally to this work.
- Supporting information and the ORCID identification number(s) for the author(s) of this article can be found under https://doi.org/10.1002/anie.202001440.

NHC-CO₂ adducts or NHC bicarbonate salts are the most common method for coating noble metal surfaces; ^[1a,4,5] however, adding NHCs to nanoparticles in aqueous solutions is more challenging. Two complementary approaches for NHC-protected nanoparticles have been developed. The free NHCs can be added directly to preformed nanoparticles ^[6] or gold NHC complexes can be reduced with borohydrides or boranes, forming NHC-functionalized gold nanoparticles (AuNPs) under 10 nm in diameter (Figure 1 a). ^[7] Yet, many applications require larger nanoparticles than can be formed with these methods. For example, in vivo biological imaging

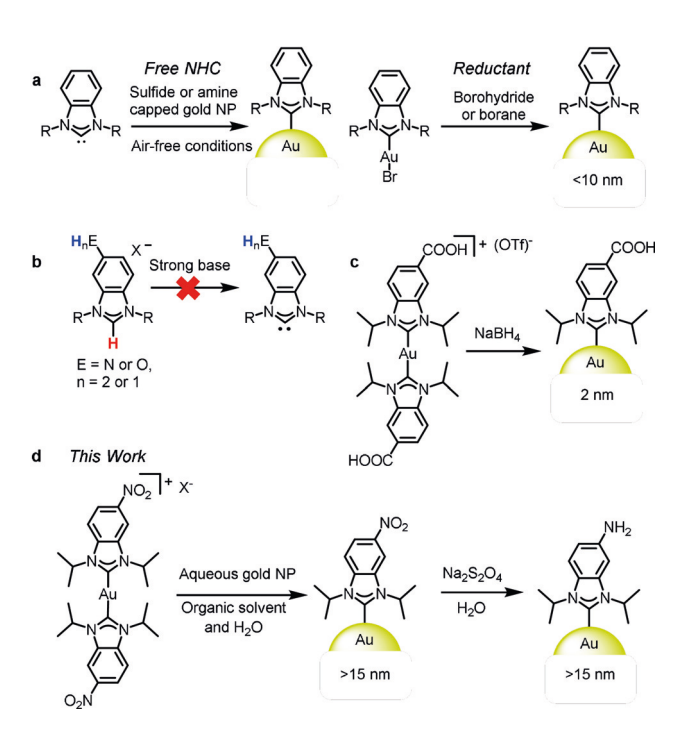
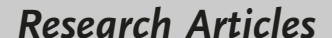


Figure 1. Synthetic schemes for NHC-functionalized surfaces and nanoparticles. a) General methods for forming NHC-capped AuNPs with aprotic functional groups. b) Forming free NHCs with protic functional groups is problematic since the protic proton (blue) is more readily deprotonated than the benzimidazolium proton. c) Crudden has formed small NPs with carboxylic acids on the backbone. [76] d) This work demonstrates a general method for formation of larger NHC-NPs with protic functional groups on the NHC. The NHC ligation is accomplished by adding a CH_2Cl_2 or CH_3CN solution of the NHC gold complex to an aqueous solution of citrate-capped nanoparticles, resulting in spontaneous functionalization. The functional groups on the NHC can be further derivatized, as shown by the nitro reduction.







require NPs greater than 10 nm to avoid rapid elimination by the kidneys^[8] and surface-enhanced Raman scattering (SERS) is most efficient with nanoparticles between 20–100 nm.^[9]

In contrast to thiols, functionalizing NHCs with protic groups is challenging. Such groups are essential as they are routinely applied in sensing, [10] biological applications, [11] and as a precursor to amide couplings. [12] While protic thiols can be added to noble metal surfaces directly, many protic functional groups, such as alcohols and amines, are incompatible with the free carbene, either due to reactions with the strong bases that are used to deprotonate the imidazolium or reactions with the free carbene itself (Figure 1 b). [13]

To date, only carboxylic acids have been employed for protic NHC-AuNPs. [3d, 7b, 14] Crudden and co-workers [7b] prepared a pendant carboxylic acid on the back of the NHC gold complex precursor prior to reduction with sodium borohydride (Figure 1c). Clearly if NHCs are to reach their full potential as versatile surface functionalization ligands, a general, straightforward method for including protic functional groups on NHC-functionalized surfaces is essential.

Results and Discussion

Herein, we report a general method for (1) creating NHC-functionalized nanoparticles (d > 15 nm) and (2) adding protic functional groups to NHC-coated surfaces (Figure 1 d). Addition of NHC gold(I) complexes to citrate-capped AuNPs (>15 nm diameter) leads to a NHC ligand replacement on the particles. As both functionalized and unfunctionalized NHCs can be transferred, this eliminates the need for NHC–CO₂ adducts, bicarbonate salts, or external reductants. Using a post synthetic modification sequence, we create NHC–amines in situ, thereby opening up amide coupling to a carboxylic acid. Each step in the synthetic sequence is followed by SERS, combined with isotope labeling and theoretical calculations, to confirm the progress of the chemical reactions on the AuNP.

We previously employed CO₂-protected NHCs to make SERS-active NHC-functionalized gold film-over-nanospheres (AuFONs); [4b,5b] however, this method of deposition is not effective for nanoparticles, except with very small atomic gold clusters. [15] The AuFONs NHCs were deposited on gold surfaces by heating the solid NHC-CO₂ compound in vacuum; therefore, this method cannot be transferred to an aqueous environment for Au nanoparticles. [4b,5b] Instead, we hypothesized that gold(I) complexes might transfer the NHC to the gold surface (Figure 2). Indeed, stirring a dilute solution of the gold(I) salt (1-I/CI) mixture of dichloromethane and water with citrate-capped nanoparticles successfully appended the NHC to the colloids without the need for an external reductant, forming 1-AuNPs.

The NHC binding to the AuNP was confirmed using SERS (Figure 3), XPS (Figure S51), and TGA (Figure S55) and the particle morphology was measured with TEM. The resulting SERS spectra are consistent with those obtained from NHC surfaces created using the NHC–CO₂ adduct method (Figure S36). [4b,5b] Peaks at 1296 cm⁻¹ and 1403 cm⁻¹

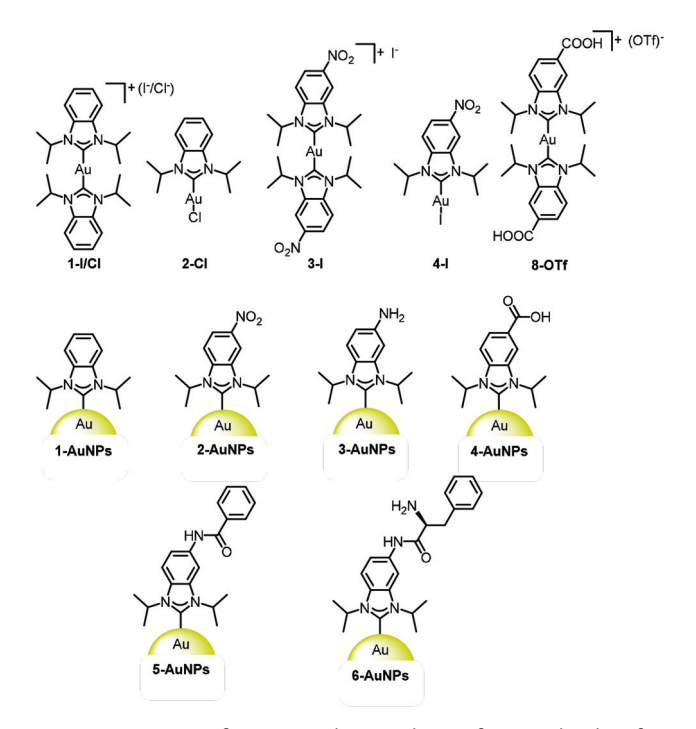


Figure 2. Summary of NHC complexes and NHC functionalized surfaces and their corresponding identifiers.

correspond to the isopropyl and aryl stretching frequencies. [16] These SERS peaks are red-shifted approximately 20 cm^{-1} relative to the Raman spectra, indicating binding to the gold surface. [5b] Several variations of our procedure all yielded **1-AuNP**: water/dichloromethane (Method 1); water/acetonitrile (Method 2); using the mono-NHC ligated gold(I) complex **2-Cl** with biphasic water/dichloromethane (Method 3). In addition, complexes with non-coordinating anions like hexafluorophosphate (PF₆) result in the same transfers of the NHC (See Figure S37). [17] Last, we observed equivalent spectra for an array of nanoparticle sizes (d = 20–100 nm), indicating formation of **1-AuNP** for a variety of initial nanoparticle substrates (See Figures S44, S45).

Deposition from the gold(I) complexes is still not amenable to the synthesis of an amine-functionalized surface due to the reactivity of the protic R-group. We reasoned that a nitro-NHC-functionalized gold surface could instead serve as the intermediate for an in situ reduction of the nitro-NHC to the amine-NHC. We, therefore, synthesized the benzimidazolium iodide precursor, 6-I, modifying our previously reported method with other functional groups, in 70% yield over two steps from 5-nitro-benzimidazole (See SI).[4b] The bis-NHC gold complexes, 3-I/Cl and 3-I, are prepared by both a strong base (Figure 4A) and a mild base approach (Figure 4B) in 95% and 71% yield, respectively. [7b] The complexes were characterized by ¹H NMR (Figures S17 and S21), HRMS (Figure S26), and X-ray crystallography (Figure S35). Additionally, the IR spectra show the characteristic 1523 and 1341 cm⁻¹ N-O stretches (Figure S25), confirming retention of the NO₂ moiety.

Given the effectiveness of the unfunctionalized mono-NHC complex, **2-Cl**, for NHC deposition, we also prepared



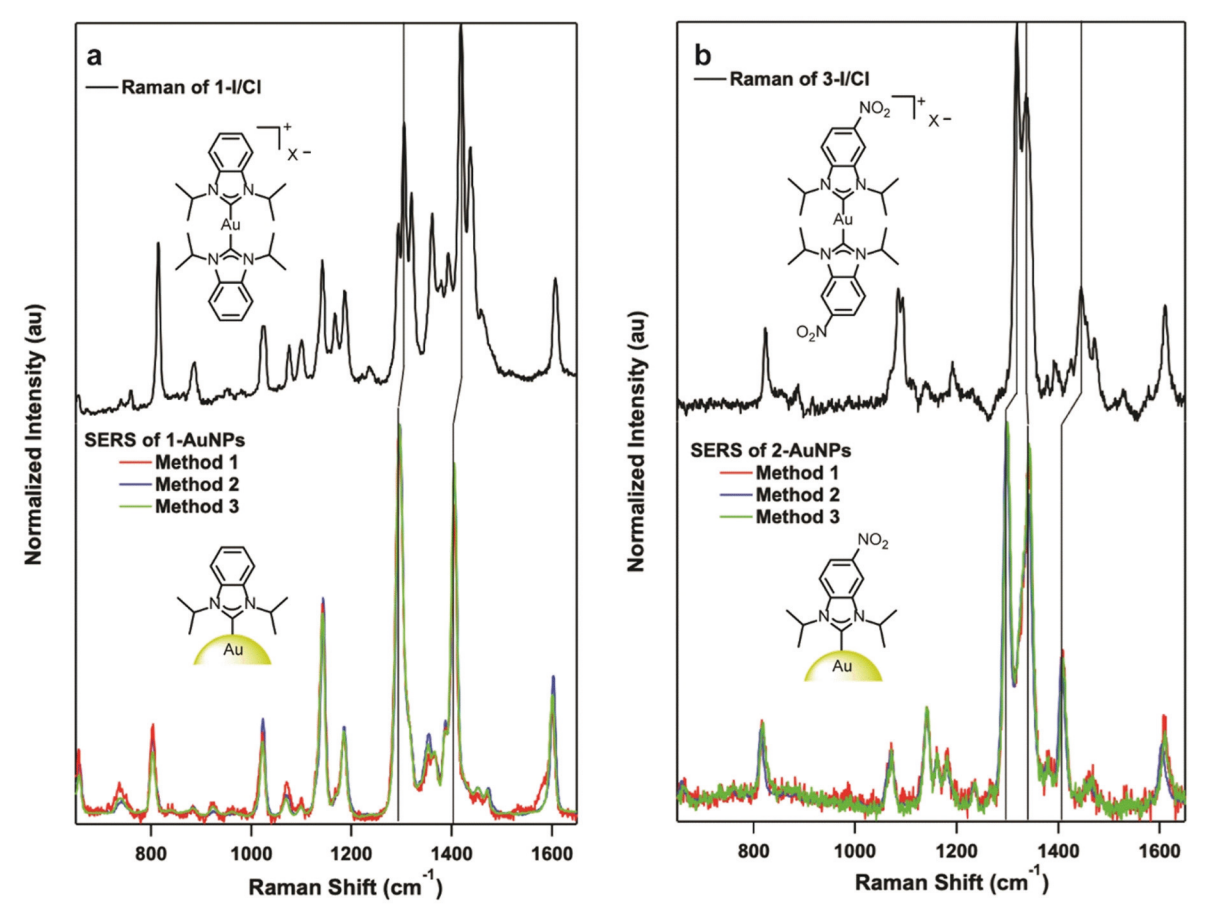


Figure 3. a) Neat Raman spectrum of 1-I/Cl (black) and SERS of 1-AuNPs. b) Neat Raman spectrum of 3-I/Cl (black) and SERS of 2-AuNPs. Three methods were used to append NHCs to the gold nanoparticles, all presenting the same signatures for 1-AuNPs: using a biphasic mixture of water and 1-1/Cl dissolved in CH₂Cl₂ (red); using a biphasic mixture of water and 1-1/Cl dissolved in CH₃CN (blue); using a biphasic mixture of water and the mono-NHC ligated gold(I) complex, 2-Cl, dissolved in CH2Cl2 (green).

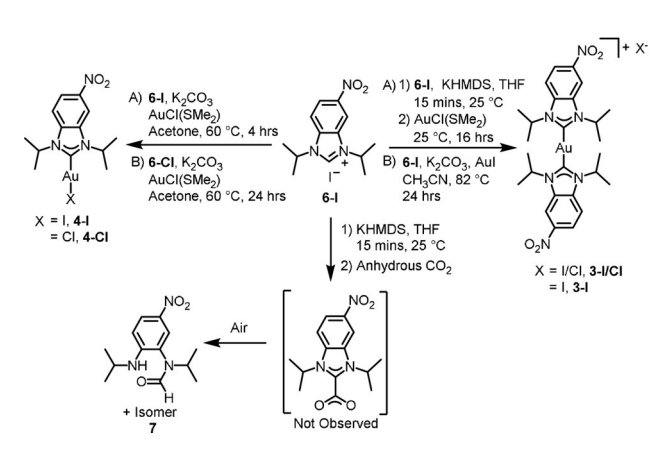


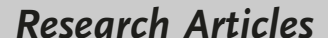
Figure 4. Synthesis of gold(I) complexes 3-I/Cl, 3-I, 4-I and 4-Cl and attempted synthesis of CO2-adduct of nitro functionalized NHC leading to decomposition product, 7.

the nitro variants. 4-I and 4-Cl were synthesized in 52% and 24% yield, respectively, from the corresponding halide salts (Figure 4, see SI for details). The gold complexes display ¹³C NMR resonances at 194.80, 191.46, and 182.03 ppm for **3**-I, 4-I, and 4-Cl (Figures S24, S28, and S32), respectively. The NHC complexes are further confirmed by HRMS (Figures S26, S30, and S34).

As before, stirring solutions of 3-I/Cl or 4-I dissolved in CH₂Cl₂ resulted in the formation of **2-AuNPs** (Figure 2). The solvent for the gold complex did not have an appreciable effect as 3-I dissolved in acetonitrile also resulted in the formation of 2-AuNPs. SERS of 2-AuNPs is comparable to 1-AuNPs with the exception of the nitro stretching band at 1342 cm⁻¹ (Figure 3b).^[18]

Our method of forming 2-AuNPs is particularly appealing because: (1) It does not require an external reductant that would reduce the nitro group prematurely.^[19] (2) The CO₂adduct for 6-I could not be prepared since it is too electron poor (Figure 4). Indeed, only the ring opened product, compound 7, was prepared (See SI). (3) The NHC transfer works for gold(I) NHC complexes with either one or two NHC ligands and different anions as well. (4) The transfer occurs under atmospheric conditions in water (with an organic co-solvent), making it a benchtop procedure. We observed spontaneous aggregation of the nanoparticles upon increasing the concentration of NHCs in solution, independent of solvent choice (See Figures S46-S50). We pose that as more ligand exchanges with the surface, the non-polar nature of the NHC induces nanoparticle aggregation, potentially

7587







limiting full displacement unless using a more hydrophilic NHC ligand. Additionally, we applied our new approach to the previously reported carboxylic acid functionalized NHC complex, **8-OTf** (shown in Figure 2), and found that transfer occurred and formed the carboxylic acid functionalized Au-NPs, **4-AuNPs**, by presence of the SERS peak at 1714 cm⁻¹ (Figure S42).^[7b] This result further reinforces that this method is general regardless of the functional group.

To further explore the addition of NHCs via the gold complexes, we collected SEM and TEM measurements of the nanoparticles before and after reaction in all solvents (Figure 5). SEM images confirmed the spectroscopic characterization ($\lambda_{\text{max}} = 521 \text{ nm}$) of the particle size, indicating AuNPs were a minimum of 12 nm and averaged 18 nm. [20] TEM analysis further confirmed that there are no obvious changes to the AuNPs size or morphology after binding, suggesting that the NHCs are binding directly to the preformed nanoparticle instead of first forming smaller aggregates (Figure 5 c and d). In addition, XPS analyses of freeze-dried 1-AuNPs yield C, N, and Au binding energies consistent with previous reports of carbene surface attachment (See Figure S51 for detailed comparison),^[21] indicating formation of the Au-NHC bond. Using the XPS atomic concentration results we also estimate the carbene ligand coverage to exceed 60%. To additionally probe the extent of surface coverage, we exposed 1-AuNPs to dodecanethiol and found that there was no obvious incorporation of the thiol (Figure S38). This experimental result implies that surface coverage by the NHCs is extensive.[2b]

We also examined NHC-functionalized nanoparticles in bulk using TGA. The TGA data is consistent with 2-Cl

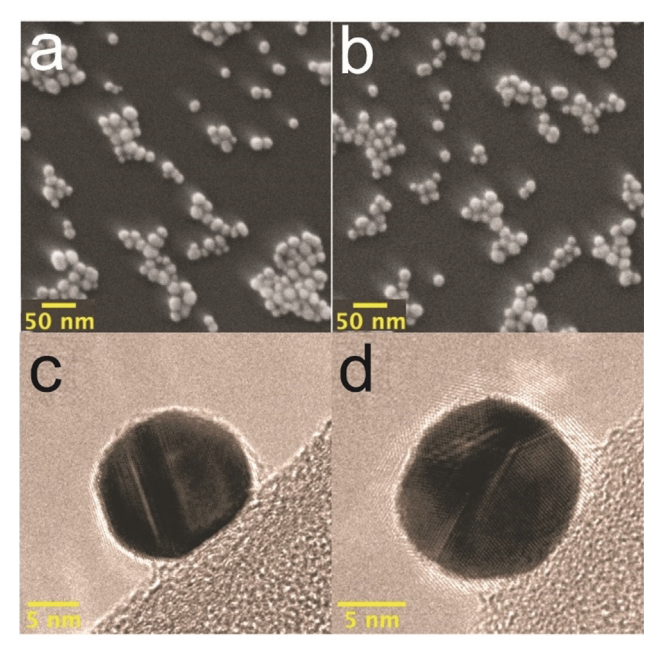


Figure 5. SEM image of AuNPs before (a) and after (b) addition of 3-1. c) TEM image of citrate-capped AuNPs before NHC functionalization. d) TEM Image of AuNPs after functionalization with 3-1 in CH_2Cl_2/H_2O . Size and shape of AuNPs stay the same before and after, suggesting that NHCs are bound directly to colloid instead of first forming small aggregates.

(Figure S53) displacing the citrate (Figure S54) and forming **1-AuNPs** (Figure S55). The lower onset temperature of **1-AuNPs** (240 °C vs. 200 °C) is a feature consistent of NHC coated AuNPs.^[22]

The amine NHC-functionalized particles, **3-AuNPs**, were achieved by reducing the nitro group on **2-AuNPs**. Initial tests with sodium borohydride degraded **2-AuNPs**, though a milder reducing agent, sodium hydrosulfite, was effective (Figure 6a). Upon reduction of the nitro-NHC, SERS analysis (Figure 6b) shows a large decrease in the NO₂ stretching band at 1342 cm⁻¹ and a simultaneous appearance of the NH₂ band at 1359 cm⁻¹. The spectrum is otherwise unperturbed, indicating the NHC is modified only at the nitro position.

To further confirm these assignments, we performed theoretical calculations of the surface-bound NH₂-NHC and we repeated the reduction in D₂O. After reduction of the nitro group in D₂O, the amine band shifts to 1347 cm⁻¹, as expected, while all other bands remain the same (Figure 6c). Density-functional theory (DFT) calculations of the SERS spectra display the same isotope effect observed in experiment. Taken together, the SERS spectra, isotope shifts, and theoretical calculations confirm the conversion of the nitro to the amine at the surface.

We finally demonstrate the functionality of the amineterminated NHCs, 3-AuNPs by performing an in situ amide coupling to a carboxylic acid, as amide coupling is a critical step for many surface and nanoparticle applications.^[23] We utilize benzoic acid here because it possesses a strong SERS active mode at 1003 cm⁻¹ that does not overlap with the NHC bands. A reaction with N,N'-diisopropylcarbodiimide (DIC) and benzoic acid in water at room temperature, followed by the addition of 3-AuNPs, formed 5-AuNPs (Figure 6a). SERS of **5-AuNPs** (Figure 6d) exhibits a strong 1000 cm⁻¹ band attributed to the benzoic acid ring mode. Importantly, no signal is observed in the ring breathing region if DIC is not added, eliminating the possibility of nonspecific biding (Figure 6d). In addition, we employed isotopic labeling to confirm amide coupling was effective. Substituting d_5 -benzoic acid led to the same spectrum except the benzoic acid peak is isotope shifted to 985 cm⁻¹. In both cases the ring stretching mode is shifted (1 cm⁻¹ for benzoic acid and 3 cm⁻¹ for d_5 benzoic acid) from the neat Raman spectra providing further evidence of the coupling.

Tethering biomolecules through amide coupling is a critical use of functionalized gold nanoparticles.^[24] To validate that the amide coupling is effective for biomolecules, we tested it with L-phenylalanine, an essential amino acid. The reaction of L-phenylalanine and DIC with **3-AuNP** yielded **6-AuNP** (see SI and Figures 2 and S43). The appearance of the same diagnostic ring stretch at 1003 cm⁻¹ as **5-AuNPs** was observed for **6-AuNP**. This result demonstrates that tethered biomolecules can be observed with SERS on these NHC-capped gold nanoparticles.

Conclusion

In conclusion, we demonstrate a general, benchtop method to append NHCs to AuNPs, resulting in the first



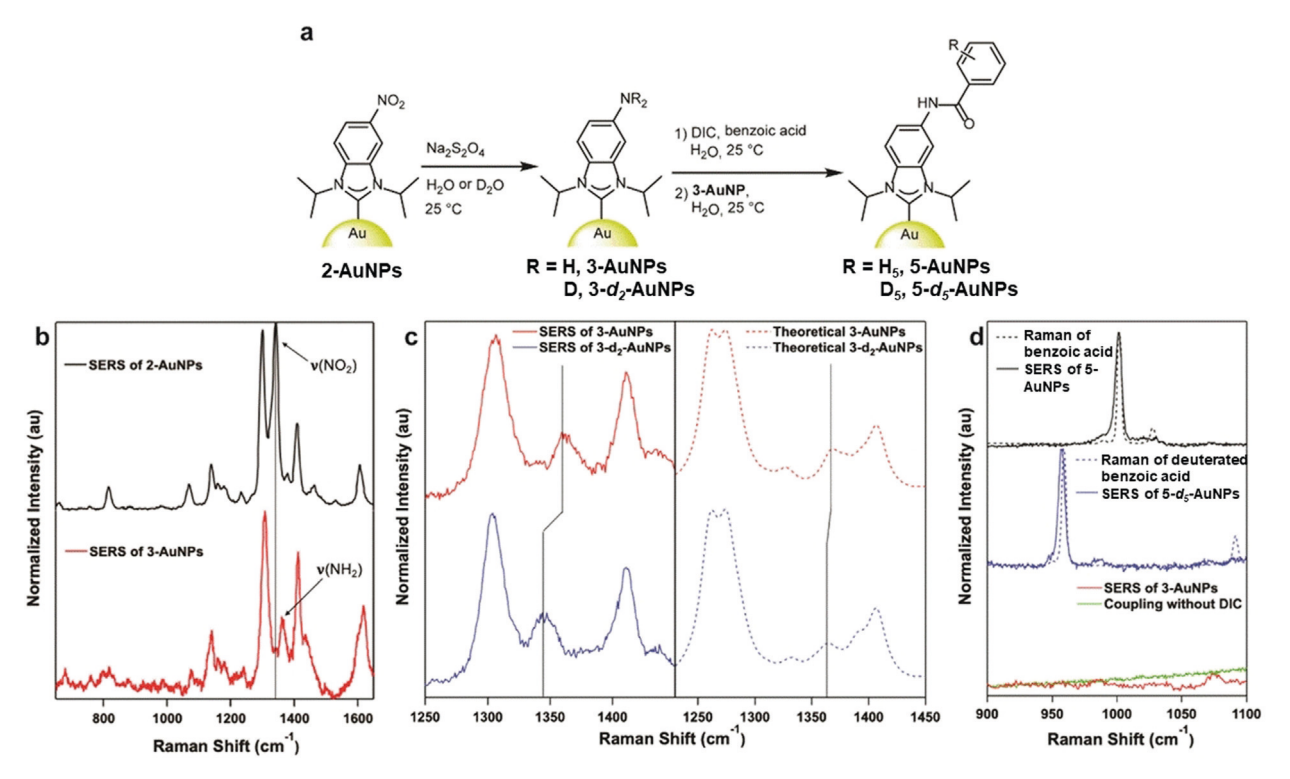


Figure 6. Formation of protic functional groups on NHC-functionalized nanoparticles via in situ post-synthetic modification. a) Reduction of 2-AuNPs to 3-AuNPs followed by amide coupling to form 5-AuNPs. b) SERS of the nitro-NHC, 2-AuNPs, (black) and amine-NHC, 3-AuNPs (red) illustrating that the nitro band disappears and the amine band appears after reduction. c) Expanded region of experimental (left, solid lines) and theoretical (right, dashed lines) SERS spectra showing the isotope shift upon reduction in either H_2O or D_2O : 3-AuNPs (red) and 3- d_2 -AuNPs (blue). d) SERS obtained after amide coupling reactions forming 5-AuNPs (black) and 5- d_5 -AuNPs (blue) compared to the neat Raman of benzoic acid (dotted black) and deuterated benzoic acid (dotted blue). SERS of controls, 3-AuNPs (red) and the coupling without DIC (green).

NHC-functionalized gold nanoparticles with d > 15 nm. Using this robust and reproducible approach, we append NHC complexes with functional groups to gold colloids across a variety of sizes. Furthermore, nitro-functionalized AuNPs were reduced in situ to form amine-functionalized NHC nanoparticles. The amine NHCs undergo an amide coupling with carboxylic acids, opening up the large space of applications afforded by the amide-linkage, including attaching biomolecules. Our approach promises to leverage the robustness of NHC gold bonds towards a plethora of new applications that were previously prohibited due to a lack of protic functional groups on the NHC backbone.

Experimental Section

All experimental and calculation details are described in the Supporting Information. Selected NMR, IR, HRMS, X-ray structures, electron microscopy images, SERS spectra, XPS analyses, and TGA plots are included. CCDC 1943496 contains the supplementary crystallographic data for this paper. These data can be obtained free of charge from The Cambridge Crystallographic Data Centre.

Acknowledgements

This material is based on work supported by the National Science Foundation under grant numbers CHE-1709881 (D.J.Y., L.M.S., and J.P.C.), CHE-1709468 (J.F.D., S.L.S, and D.M.J.), CHE-1362825, and NRT-1449785 (J.C.B., and L.J.). L.F.P.K. thanks the German Academic Exchange Service for funding. Any opinions, findings, and conclusions or recommendations expressed in this material are those of the authors and do not necessarily reflect the views of the National Science Foundation. Portions of this work were conducted with Advanced Cyberinfrastructure computational resources provided by The Institute for Cyber-Science at The Pennsylvania State University (http://ics.psu.edu). J.P.C., D.J.Y., and S.L.S., wish to thank John Dunlap for assistance with the SEM and TEM measurements. J.P.C. and L.M.S. thank the ND Energy Materials Characterization Facility (MCF) for assistance with the XPS experiments. The MCF is funded by the Sustainable Energy Initiative (SEI), which is part of the Center for Sustainable Energy at Notre Dame (ND Energy). J.F.D. and D.M.J. thank the Brantley group at the University of Tennessee for access to their laboratory TGA instrument.

Conflict of interest

The authors declare no conflict of interest.

Research Articles





Keywords: gold \cdot nanoparticles \cdot N-heterocyclic carbenes \cdot SERS \cdot surface modification

How to cite: Angew. Chem. Int. Ed. **2020**, 59, 7585–7590 Angew. Chem. **2020**, 132, 7655–7660

- a) C. M. Crudden, J. H. Horton, M. R. Narouz, Z. Li, C. A. Smith, K. Munro, C. J. Baddeley, C. R. Larrea, B. Drevniok, B. Thanabalasingam, A. B. McLean, O. V. Zenkina, I. I. Ebralidze, Z. She, H.-B. Kraatz, N. J. Mosey, L. N. Saunders, A. Yagi, Nat. Commun. 2016, 7, 12654; b) D. J. Lavrich, S. M. Wetterer, S. L. Bernasek, G. Scoles, J. Phys. Chem. B 1998, 102, 3456-3465.
- [2] a) C. A. Smith, M. R. Narouz, P. A. Lummis, I. Singh, A. Nazemi, C.-H. Li, C. M. Crudden, Chem. Rev. 2019, 119, 4986 5056; b) C. M. Crudden, J. H. Horton, I. I. Ebralidze, O. V. Zenkina, A. B. McLean, B. Drevniok, Z. She, H.-B. Kraatz, N. J. Mosey, T. Seki, E. C. Keske, J. D. Leake, A. Rousina-Webb, G. Wu, Nat. Chem. 2014, 6, 409; c) S. Qi, Q. Ma, X. He, Y. Tang, Colloids Surf. A 2018, 538, 488 493; d) D. T. Nguyen, M. Freitag, M. Körsgen, S. Lamping, A. Rühling, A. H. Schäfer, M. H. Siekman, H. F. Arlinghaus, W. G. van der Wiel, F. Glorius, B. J. Ravoo, Angew. Chem. Int. Ed. 2018, 57, 11465 11469; Angew. Chem. 2018, 130, 11637 11641; e) M.-T. Lee, C.-C. Hsueh, M. S. Freund, G. S. Ferguson, Langmuir 1998, 14, 6419 6423.
- [3] a) Z. Li, K. Munro, M. R. Narouz, A. Lau, H. Hao, C. M. Crudden, J. H. Horton, ACS Appl. Mater. Interfaces 2018, 10, 17560-17570; b) Z. Li, M. R. Narouz, K. Munro, B. Hao, C. M. Crudden, J. H. Horton, H. Hao, ACS Appl. Mater. Interfaces 2017, 9, 39223-39234; c) Z. Li, K. Munro, I. I. Ebralize, M. R. Narouz, J. D. Padmos, H. Hao, C. M. Crudden, J. H. Horton, Langmuir 2017, 33, 13936-13944; d) A. Ferry, K. Schaepe, P. Tegeder, C. Richter, K. M. Chepiga, B. J. Ravoo, F. Glorius, ACS Catal. 2015, 5, 5414 – 5420; e) Z. Cao, D. Kim, D. Hong, Y. Yu, J. Xu, S. Lin, X. Wen, E. M. Nichols, K. Jeong, J. A. Reimer, P. Yang, C. J. Chang, J. Am. Chem. Soc. 2016, 138, 8120-8125; f) J. B. Ernst, C. Schwermann, G.-i. Yokota, M. Tada, S. Muratsugu, N. L. Doltsinis, F. Glorius, J. Am. Chem. Soc. 2017, 139, 9144-9147; g) P. Tegeder, M. Freitag, K. M. Chepiga, S. Muratsugu, N. Möller, S. Lamping, M. Tada, F. Glorius, B. J. Ravoo, Chem. Eur. J. 2018, 24, 18682-18688.
- [4] a) A. V. Zhukhovitskiy, M. G. Mavros, T. Van Voorhis, J. A. Johnson, J. Am. Chem. Soc. 2013, 135, 7418-7421; b) J. F. DeJesus, M. J. Trujillo, J. P. Camden, D. M. Jenkins, J. Am. Chem. Soc. 2018, 140, 1247-1250.
- [5] a) G. Wang, A. Rühling, S. Amirjalayer, M. Knor, J. B. Ernst, C. Richter, H.-J. Gao, A. Timmer, H.-Y. Gao, N. L. Doltsinis, F. Glorius, H. Fuchs, *Nat. Chem.* 2016, 9, 152; b) M. J. Trujillo, S. L. Strausser, J. C. Becca, J. F. DeJesus, L. Jensen, D. M. Jenkins, J. P. Camden, *J. Phys. Chem. Lett.* 2018, 9, 6779–6785.
- [6] a) E. C. Hurst, K. Wilson, I. J. S. Fairlamb, V. Chechik, New J. Chem. 2009, 33, 1837–1840; b) R. W. Y. Man, C.-H. Li, M. W. A. MacLean, O. V. Zenkina, M. T. Zamora, L. N. Saunders, A. Rousina-Webb, M. Nambo, C. M. Crudden, J. Am. Chem. Soc. 2018, 140, 1576–1579.
- [7] a) X. Ling, N. Schaeffer, S. Roland, M.-P. Pileni, Langmuir 2013, 29, 12647–12656; b) K. Salorinne, R. W. Y. Man, C.-H. Li, M. Taki, M. Nambo, C. M. Crudden, Angew. Chem. Int. Ed. 2017, 56, 6198–6202; Angew. Chem. 2017, 129, 6294–6298; c) M. J. MacLeod, J. A. Johnson, J. Am. Chem. Soc. 2015, 137, 7974–7977.
- [8] N. Hoshyar, S. Gray, H. Han, G. Bao, Nanomedicine 2016, 11, 673-692

- [9] N. D. Israelsen, C. Hanson, E. Vargis, Sci. World J. 2015, 12.
- [10] a) B. Sharma, P. Bugga, L. R. Madison, A.-I. Henry, M. G. Blaber, N. G. Greeneltch, N. Chiang, M. Mrksich, G. C. Schatz, R. P. Van Duyne, J. Am. Chem. Soc. 2016, 138, 13952-13959;
 b) C. Zhang, X. Liang, T. You, N. Yang, Y. Gao, P. Yin, Anal. Methods 2017, 9, 2517-2522;
 c) X. Gu, H. Wang, Z. D. Schultz, J. P. Camden, Anal. Chem. 2016, 88, 7191-7197;
 d) O. Lyandres, N. C. Shah, C. R. Yonzon, J. T. Walsh, M. R. Glucksberg, R. P. Van Duyne, Anal. Chem. 2005, 77, 6134-6139.
- [11] a) Y. Zhao, Y. Tian, Y. Cui, W. Liu, W. Ma, X. Jiang, J. Am. Chem. Soc. 2010, 132, 12349–12356; b) X. Li, S. M. Robinson, A. Gupta, K. Saha, Z. Jiang, D. F. Moyano, A. Sahar, M. A. Riley, V. M. Rotello, ACS Nano 2014, 8, 10682–10686.
- [12] a) T. Zhang, P. Chen, Y. Sun, Y. Xing, Y. Yang, Y. Dong, L. Xu, Z. Yang, D. Liu, *Chem. Commun.* 2011, 47, 5774-5776; b) C. M. Alexander, K. L. Hamner, M. M. Maye, J. C. Dabrowiak, *Bioconjugate Chem.* 2014, 25, 1261-1271; c) L. He, M. Langlet, V. Stambouli, *Appl. Surf. Sci.* 2017, 399, 702-710.
- [13] a) S. Kuwata, F. E. Hahn, Chem. Rev. 2018, 118, 9642-9677;
 b) W. W. N. O, A. J. Lough, R. H. Morris, Organometallics 2009, 28, 6755-6761;
 c) W. W. N. O, A. J. Lough, R. H. Morris, Chem. Commun. 2010, 46, 8240-8242;
 d) D. Enders, K. Breuer, G. Raabe, J. Runsink, J. H. Teles, J.-P. Melder, K. Ebel, S. Brode, Angew. Chem. Int. Ed. Engl. 1995, 34, 1021-1023; Angew. Chem. 1995, 107, 1119-1122.
- [14] D. A. Lomelí-Rosales, I. I. Rangel-Salas, A. Zamudio-Ojeda, G. G. Carbajal-Arízaga, C. Godoy-Alcántar, R. Manríquez-González, J. G. Alvarado-Rodríguez, D. Martínez-Otero, S. A. Cortes-Llamas, ACS Omega 2016, 1, 876–885.
- [15] M. R. Narouz, K. M. Osten, P. J. Unsworth, R. W. Y. Man, K. Salorinne, S. Takano, R. Tomihara, S. Kaappa, S. Malola, C.-T. Dinh, J. D. Padmos, K. Ayoo, P. J. Garrett, M. Nambo, J. H. Horton, E. H. Sargent, H. Häkkinen, T. Tsukuda, C. M. Crudden, *Nat. Chem.* 2019, 11, 419–425.
- [16] X. Ren, E. Tan, X. Lang, T. You, L. Jiang, H. Zhang, P. Yin, L. Guo, Phys. Chem. Chem. Phys. 2013, 15, 14196–14201.
- [17] H. Sivaram, J. Tan, H. V. Huynh, Organometallics 2012, 31, 5875-5883.
- [18] C. Passingham, P. J. Hendra, C. Hodges, H. A. Willis, Spectrochim. Acta Part A 1991, 47, 1235–1245.
- [19] a) S. Fountoulaki, V. Daikopoulou, P. L. Gkizis, I. Tamiolakis, G. S. Armatas, I. N. Lykakis, ACS Catal. 2014, 4, 3504-3511;
 b) M. J. MacLeod, A. J. Goodman, H.-Z. Ye, H. V. T. Nguyen, T. Van Voorhis, J. A. Johnson, Nat. Chem. 2019, 11, 57-63.
- [20] P. C. Lee, D. Meisel, J. Phys. Chem. 1982, 86, 3391 3395.
- [21] a) N. Bridonneau, L. Hippolyte, D. Mercier, D. Portehault, M. Desage-El Murr, P. Marcus, L. Fensterbank, C. Chanéac, F. Ribot, *Dalton Trans.* 2018, 47, 6850–6859; b) G. Wang, A. Rühling, S. Amirjalayer, M. Knor, J. B. Ernst, C. Richter, H.-J. Gao, A. Timmer, H.-Y. Gao, N. L. Doltsinis, F. Glorius, H. Fuchs, *Nat. Chem.* 2017, 9, 152–156.
- [22] M. R. Narouz, C.-H. Li, A. Nazemi, C. M. Crudden, *Langmuir* 2017, 33, 14211–14219.
- [23] M. Fèvre, J. Pinaud, A. Leteneur, Y. Gnanou, J. Vignolle, D. Taton, K. Miqueu, J.-M. Sotiropoulos, J. Am. Chem. Soc. 2012, 134, 6776–6784.
- [24] J. Conde, J. T. Dias, V. Grazú, M. Moros, P. V. Baptista, J. M. de la Fuente, *Front. Chem.* 2014, https://doi.org/10.3389/fchem. 2014.00048.

Manuscript received: January 28, 2020 Accepted manuscript online: February 24, 2020 Version of record online: March 12, 2020